

## Characterization of HSCD5, a novel human stearoyl-CoA desaturase unique to primates

Jian Wang<sup>a,\*</sup>, Lan Yu<sup>a</sup>, Robert E. Schmidt<sup>a</sup>, Chen Su<sup>b</sup>, Xiaodi Huang<sup>a</sup>,  
Kenneth Gould<sup>a</sup>, Guoqing Cao<sup>a</sup>

<sup>a</sup> Cardiovascular Division, Lilly Research Labs, Eli Lilly and Company, DC 0343, Indianapolis, IN 46285, USA

<sup>b</sup> Integrative Biology, Lilly Research Labs, Eli Lilly and Company, DC 0343, Indianapolis, IN 46285, USA

Received 2 May 2005

Available online 12 May 2005

### Abstract

Stearoyl-CoA desaturase (SCD) is an integral membrane protein of the endoplasmic reticulum (ER) that catalyzes the formation of monounsaturated fatty acids from saturated fatty acids. Recent studies suggest that SCD is a key regulator of energy metabolism and has implications in dislipidemia and obesity. Four SCD isoforms (SCD1–4) have been identified in mouse. In human, only one SCD isoform has been characterized so far. Here we report that the previously reported human ACOD4 gene encodes a distinct stearoyl-CoA desaturase, hSCD5. GenBank database mining revealed orthologues of hSCD5 in the primates, but not in the rodents. In transiently transfected 293 cells, hSCD5 co-localized with calnexin on ER membrane. Microsome fractions prepared from hSCD1 and hSCD5 transfected cells displayed similar delta 9 desaturase activity. Quantitative real-time RT-PCR analysis suggested that hSCD5 was abundantly expressed in adult brain and pancreas. These data suggested that hSCD5 plays a role distinct from that of hSCD1 during development and in normal physiological conditions.

© 2005 Elsevier Inc. All rights reserved.

**Keywords:** Stearoyl-CoA desaturase; Gene expression; SCD isoform

In mammalian systems, monounsaturated fatty acids are formed by the direct oxidative desaturation (the removal of two hydrogens resulting in the introduction of a double bond) of long chain saturated fatty acyl-Coenzyme A at the delta 9 position [1]. The mammalian delta 9 desaturation system consists of three endoplasmic reticulum (ER) membrane protein components: (1) NADH-cytochrome *b5* reductase, (2) cytochrome *b5*, and (3) a desaturase protein. The delta 9 desaturase protein has over 62% of non-polar amino acid residues and is largely embedded in ER membrane, with active sites exposed to the cytosol. Site-directed mutagenesis study confirmed that clusters of histidine-rich motifs are required for catalytic activity [2,3]. The preferred sub-

strates for SCD are palmitoyl-CoA and stearoyl-CoA, which are converted into palmitoleoyl-CoA and oleoyl-CoA, respectively. Thus, the mammalian delta 9 desaturase is also called stearoyl-CoA desaturase (SCD).

Monounsaturated fatty acids play multiple critical physiological roles in living organisms [4,5]. Oleic acid is the most abundant fatty acid in membrane phospholipids, triglycerides, cholesterol esters, and wax esters. Mice deficient of mSCD1 displayed impaired hepatic triglyceride biosynthesis and much lower plasma very low-density lipoprotein (VLDL) and plasma triglyceride levels. These mice are also resistant to diet-induced weight gain and diabetes, probably mediated through multiple mechanisms including reduced expression of lipogenic enzymes, elevated AMP-activated protein kinase activities, and increased metabolic rate [6,7]. Hepatic SCD1 expression is regulated by many hormonal

\* Corresponding author.

E-mail address: [jyw@lilly.com](mailto:jyw@lilly.com) (J. Wang).

factors including insulin and leptin. SCD1 is a major peripheral target of leptin, a key regulator of energy homeostasis and satiety. SCD1 null mice displayed attenuated obesity phenotype in leptin deficiency background [8]. SCD1 may also play a role in cholesterol efflux process. It has been shown that monounsaturated fatty acids induce SCD1 expression and ABCA1 degradation in human macrophage cells [9,10]. Inhibition of SCD activity blocked the ABCA1 degradation and enhanced high-density lipoprotein (HDL)-mediated cholesterol efflux. Human epidemiology studies demonstrated a reverse correlation between hepatic SCD activity and plasma HDL level [11]. Sequence variation in SCD1 gene is also linked to susceptibility of developing type 2 diabetes [12]. Taken together, these data suggested SCD1 as a potential therapeutic target for multiple metabolic diseases including dyslipidemia, obesity, and type 2 diabetes.

Four SCD isoforms have been characterized in the mice [4,13]. These four isoforms displayed similar desaturation activities towards stearoyl-CoA and palmitoyl-CoA but have different tissue distributions. Mouse SCD1 is ubiquitously expressed with the highest expression detected in liver, adipose tissue, preputial gland, and harderian gland. Expression of mSCD1 in adipose tissue appears to be constitutive while hepatic mSCD1 expression is regulated by multiple dietary and hormonal factors. Highest mSCD2 expression was detected in brain and harderian gland while mSCD3 expression is limited to harderian gland. The recently identified mouse SCD4 appears to be heart specific.

In humans, only one SCD isoform has been well characterized so far. This appears to be the human orthologue of mouse SCD1. Here, we report the characterization of a novel human SCD isoform, which we have termed hSCD5. The gene encoding hSCD5 was previously cloned as ACOD4 from the chromosome inversion site in a family with cleft lip [14]. We show here that ACOD4 encodes a functional delta 9 desaturase and is localized on ER membrane. However, it is not the orthologue of any of the four mice SCD genes based on our phylogenetic analysis for all mammalian SCD proteins. Real-time RT-PCR analysis indicated that hSCD5 is highly expressed in brain and pancreas.

## Experimental procedures

**Identification and cloning of human SCD5.** A comprehensive BLAST search was conducted using predicted amino acid sequences of human SCD1 (hSCD1: NP\_005054), mouse SCD1 (mSCD1, NP\_033153), and mSCD4 (NP\_899039) against the human nucleotide database. This resulted in over 20 human cDNA and EST sequences displaying significant homology to human and mouse SCDs. Multiple alignment and sequence comparison of these nucleotide sequences revealed that they are derived from either human SCD1 mRNA or a

previously reported novel acyl-CoA desaturase gene disrupted in a family with cleft lip (ACOD4, AF389338). In the National Center for Biotechnology Information (NCBI) database, this gene is termed as human SCD4. However, sequence analysis suggested that AF389338 is not the human orthologue of mouse SCD4.

The coding region of AF389338 was cloned from a human brain cDNA library (BD Biosciences, Palo Alto, CA) by PCR amplification using primers with sequences: 5'-CCAGCCATCGGAGGC and 5'-ATGTGGGATGGCTGTTC. The amplified cDNA was purified from gel and cloned into pGem-T vector (Promega, Madison, WI). The coding region of hSCD5 was subsequently cloned into mammalian expression vector pcDNA3.1 (Invitrogen, Carlsbad, CA) to generate pcDNA-hSCD5. To generate N-terminal green fluorescent protein (GFP)-hSCD5 fusion protein, hSCD5 was subcloned into pEGFP vectors (BD Biosciences, Palo Alto, CA). The resulting construct was named pEGFP-hSCD5. Likewise, hSCD1 cDNA was amplified from a human liver cDNA library (BD Biosciences) by PCR using primers with sequences: 5'-GCTACTTGTCTTTTTCGAAAGCTTGG and 5'-GCGGATCCACTCTTGTAGTTTCATCTCC. Mammalian expression constructs pcDNA3-hSCD1 and pEGFP-hSCD1 were established in a similar manner.

**Microsome fraction preparation and delta 9 desaturase assay.** Human embryonic kidney (NEK) 293 cells grown on Petri dish were transiently transfected with plasmid DNA encoding hSCD1, hSCD5 or empty vector alone. Forty-eight hours after transfection, cells were washed with phosphate-buffered saline (PBS) and harvested with a cell scraper. Cell pellets were re-suspended in buffer A (50 mM Tris, pH 7.5, 250 mM sucrose, 1 mM EDTA, and 0.1 mM DTT) and cells were disrupted with brief sonication. The microsome fraction (100,000g) was isolated by sequential centrifugation and re-suspended in buffer A. Protein concentration was determined with the Bradford method and stored at  $-80^{\circ}\text{C}$  until use.

The thin layer chromatography (TLC) method was employed for the measurement of desaturase activity [15]. The final reaction mixture contained 100 mM potassium phosphate buffer, pH 7.2, 0.1 mM EDTA, 0.1 mM DTT, 1 mM NADH, 0.1 mM ATP, 0.2 mM coenzyme A, and 20  $\mu\text{g}$  of microsome prep in a total volume of 95  $\mu\text{l}$ . To this mixture, 5  $\mu\text{l}$  of substrate mix containing 0.2  $\mu\text{Ci}$   $^{14}\text{C}$ -labeled stearoyl-CoA (55  $\mu\text{Ci}/\mu\text{mol}$ , ARC, St. Louis, MO) was added to initiate the reaction. The reaction was terminated by the addition of 100  $\mu\text{l}$  of 2.5 M KOH in methanol and fatty acids extracted with hexane, methylated by the addition of 10% acetic chloride/methanol, and incubated at  $85^{\circ}\text{C}$  for 60 min. The saturated and monounsaturated fatty acid methyl esters were separated by 10%  $\text{AgNO}_3$ -impregnated TLC using hexane/diethyl ether (9:1) as developing solution. Following chromatography, the plate was dried in air and exposed to a Phosphorimage screen. A Storm phosphorimager was used to visualize and quantify the  $^{14}\text{C}$ -labeled fatty acids. Band intensities corresponding to saturated and monounsaturated fatty acids were used to calculate the percentage of conversion and enzyme activity.

**Immunoblotting and immunohistochemistry.** For immunoblotting analysis, microsome fractions (30  $\mu\text{g}$ ) from pEGFP-hSCD1, pEGFP-hSCD5 or mock-transfected 293 cells were mixed with the 2 $\times$  sodium dodecyl sulfate (SDS) sample buffer (Novex, San Diego, CA), separated on a pre-cast SDS-10% polyacrylamide gel (Novex), and transferred to nylon membranes. Membranes were probed with monoclonal antibody against GFP (BD Biosciences, Palo Alto, CA) followed with horseradish peroxidase (HRP) conjugated secondary antibody (Santa Cruz, CA). Membranes were developed with the enhanced chemiluminescent reagent (Amersham Biosciences, Piscataway, NJ) and exposed to X-ray film.

For the subcellular localization of hSCD1 and hSCD5, 293 cells cultured on cover-slides were transiently transfected with pEGFP-hSCD1 or pEGFP-hSCD5. Twenty-four hours after transfection, the cells were fixed with 2% formaldehyde for 1 min and permeabilized with 0.2% Triton X-100 in phosphate-buffered saline (PBS) with 2% BSA (bovine albumin fraction V, Life Technologies, MD).

Samples were washed with PBS three times before incubation with calnexin antibody (Affinity BioReagents, CA). After overnight incubation with the calnexin antibody at 1:500 dilutions in PBS-BSA, secondary antibody (Alexa Fluor 674-checken anti-mouse IgG, Molecular Probes, OR) was added at 1:500 dilution. Following 1-h incubation with secondary antibody, samples were washed and sealed with a coverslip using GEL/MOUNT (Molecular Probes).

The Images were collected on an MRC1024-UV Confocal System (Bio-Rad) equipped with a 40 Plan Apo, oil immersion objective on a Diaphot 200 inverted microscope (Nikon). Dual channel scanning was used to acquire fluorescent signals from GFP and Alexa Fluor 674. The green and red fluorescent images were collected sequentially with Lasersharp 2000 (Bio-Rad) acquisition software. To enhance the signal-to-noise ratio, Kalman averaging option was applied (three scans).

**Quantitative RT-PCR.** Total RNA from multiple human tissues was purchased from Clontech (Life Technologies, MD). RNA samples were treated with DNase I and extracted with phenol/chloroform to remove any contaminating genomic DNA. The first strand cDNA was prepared by reverse transcription with 2  $\mu$ g RNA in a 20  $\mu$ l reaction volume using the Superscript II kit (Life Technologies). Quantitative sequence detection was carried out on an ABI PRISM 7700 instrument (Applied Biosystems, Foster City, CA) using standard conditions. The universal PCR mix, and primers and probes for glyceraldehyde-3-phosphate dehydrogenase (GAPDH) were from Applied Biosystems. The nucleotide probes and primers for hSCD1 and hSCD5 were designed using Primer Express version 2.0 (Applied Biosystems) and were synthesized by Biosource International (Camarillo, CA). Primer and probe sequences (hSCD1 forward: GTACCGCTGGCACATCAA CTT; hSCD1 reverse: TTGGAGACTTTCTTCCGGTCAT; hSCD1 probe: CATTCTTCATTGATTGCATGGCCGC; hSCD5 forward: GGCAACCAAGCCGATGATC; hSCD5 reverse: GTGGGATGGC TGTTCCAAGT; hSCD5 probe: AGGCCCGGAAGGCCAGGA CTG) were searched against NCBI database to ensure the target specificity. The relative expression levels of a specific gene in each sample were calculated using comparative  $C_t$  method, where  $\Delta C_t = \text{unkn } C_t - \text{GAPDH } C_t$ , and  $\Delta\Delta C_t = \text{unkn1 } \Delta C_t - \text{unkn2 } \Delta C_t$ .

**Evolutionary genetic analysis.** The phylogenetic analysis was performed using Molecular Evolutionary Genetic Analysis software; MEGA version 2.1 [16], available at <http://www.megasoftware.net>. The following amino acid sequences were included in the phylogenetic tree reconstruction: bovine SCD1 (GenBank Accession No. AAF22305.1), chimpanzee SCD1 (XP\_507982.1), chimpanzee SCD5 (XP\_517188.1), goat SCD1 (AAK01666.1), hamster SCD (AAC42058.1), human SCD1 (CAA73998.1), human SCD5 (AAP31443.1), mouse SCD1 (AAA40103.1), mouse SCD2 (AAH40384.1), mouse SCD3 (NP\_077770.1), mouse SCD4 (AAR06950.1), orangutan SCD1 (CAH91238.1), orangutan SCD5 (CAH90151.1), rat SCD1 (AAM34746.1), rat SCD2 (AAH61737.1), sheep SCD1 (NP\_001009254.1), and swine SCD1 (NP\_998946.1).

The amino acid alignment was performed using the Clustal W computer program [17], followed by manual adjustment. A neighbor-joining tree [18] with Poisson distance was constructed and the statistical significance of the tree was assessed by the bootstrap method [19] with 500 replicates.

## Results

### *Human SCD5 is a stearyl-CoA desaturase unique to primates*

In the NCBI database, ACOD4 (GenBank Accession No. AF389338) is termed as human SCD4. To determine if this is the human orthologue of mouse SCD4, we performed multiple alignments with the predicted amino acid sequences of human SCD1, AF389338, mouse SCD1 (mSCD1), mouse SCD2 (mSCD2), mouse SCD3 (mSCD3), mouse SCD4 (mSCD4), rat SCD1 (rSCD1), and rat SCD2 (rSCD2). As shown in Table 1, there are 79–87% identities among these SCD isoforms except AF389338. When conserved amino acids are considered, there are 91–98% similarities among these SCD isoforms excluding AF389338. In contrast, AF389338 only shared 54–58% identity and 72–74% similarity with other SCD isoforms. These data suggested that AF389338 is not the human orthologue of mSCD4. Rather, it encodes a novel human stearyl-CoA desaturase distinct from all four mouse SCDs. Therefore, we termed it as human SCD5.

Extensive BLAST search using the amino acid sequence of hSCD5 against mouse and rat genomic and cDNA database did not reveal the orthologue of hSCD5 in these two species. Considering the fact that the mouse genomic sequence is complete, we concluded that the orthologue of hSCD5 does not exist in mouse. More BLAST search revealed two potential hSCD5 orthologues in two other primate species, orangutan (*Pongo pygmaeus*) and chimpanzee (*Pan troglodytes*). No other hSCD5 orthologue was found in other species.

Fig. 1A shows the predicted amino acid sequence alignment of SCD5 from the three primates. The orangutan SCD5 (CAH90151) contains 256 amino acids and

Table 1  
Homology of the predicted amino acid sequences of human, mouse, and rat SCDs

% similarity	% identity							
	hSCD1	hSCD5	mSCD1	mSCD2	mSCD3	mSCD4	rSCD1	rSCD2
hSCD1		74.5	94.1	91.3	93.0	88.7	95.0	92.2
hSCD5	58.2		74.5	73.9	74.5	72.1	75.8	74.5
mSCD1	84.8	57.9		91.5	93.8	87.0	96.9	92.1
mSCD2	82.7	57.0	86.5		91.9	92.7	92.7	98.9
mSCD3	82.7	56.7	88.7	84.9			94.1	92.5
mSCD4	78.2	54.5	80.2	79.6	79.3		88.7	86.4
rSCD1	84.9	58.5	93.2	85.2	82.7	82.7		93.3
rSCD2	83.5	57.6	87.0	96.1	85.8	81.3	87.2	

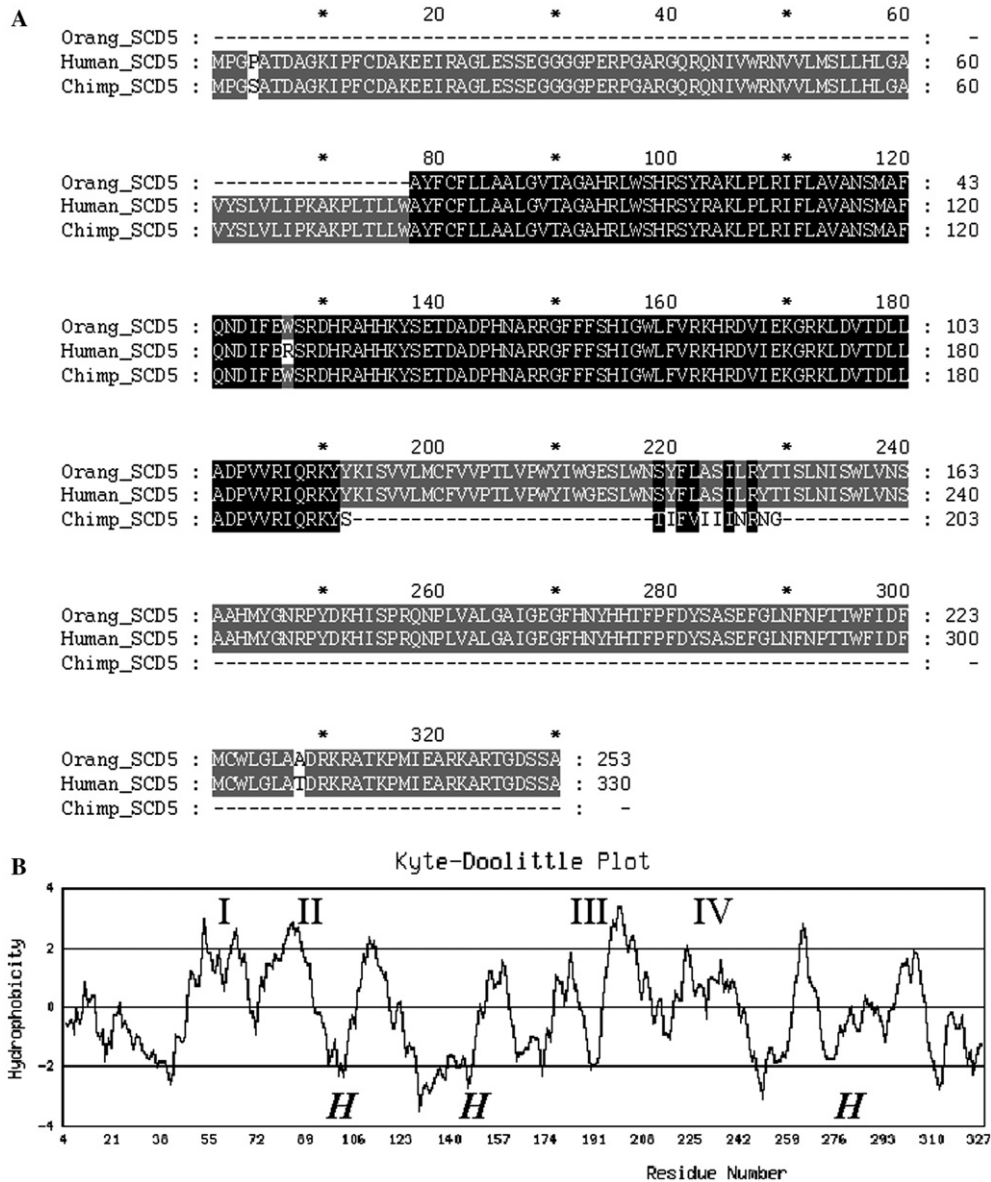


Fig. 1. (A) Alignment of the predicted amino acid sequence of SCD5 from human, chimpanzee, and orangutan. Shaded areas represent identical amino acids. (B) Kyte and Doolittle plot of the predicted human SCD5 protein. The positive score is proportional to the degree of hydrophobicity. The four trans-membrane domains are labeled I–VI and the histidine motifs are denoted H.

was deduced from a cDNA clone (CR857900) from the German cDNA Consortium. The chimpanzee SCD5 (XP\_517188) has 199 amino acids and was derived from a cDNA (NW\_105918) predicted from the chimpanzee genomic sequences. The orangutan and chimpanzee SCD5 cDNA sequences are likely partial with orangutan SCD5 missing the N-terminal 69 amino acids and chimpanzee SCD5 missing the C-terminal 131 amino acids. Nevertheless, they are 98.8% and 96.0% identical to hSCD5, suggesting that they represent true orthologues of human SCD5. Kyte–Doolittle plot (Fig. 1B) of the predicted amino acid sequence of hSCD5 revealed four trans-membrane domains, similar to other SCD isoforms. The three histidine clusters important to fatty-acyl desaturase activity are also conserved.

#### *Delta 9 desaturase activity and subcellular localization*

To determine whether hSCD5 encodes a functional delta 9 desaturase, mammalian expression vectors (pcDNA3.1) encoding hSCD1 and hSCD5 were constructed. It was reported that GFP-SCD1 fusion protein displayed similar SCD activity as wild type SCD1. Therefore, vectors encoding GFP-hSCD1 and GFP-hSCD5 fusion protein were also constructed. Microsome fractions were prepared from 293 cells transiently transfected with these vectors and Western blot analysis with a GFP antibody revealed a similar level expression of the fusion proteins (Fig. 2C). Delta 9 desaturase activity towards  $^{14}\text{C}$ -labeled stearoyl-CoA was measured using the TLC method. As shown in Fig. 2, micro-

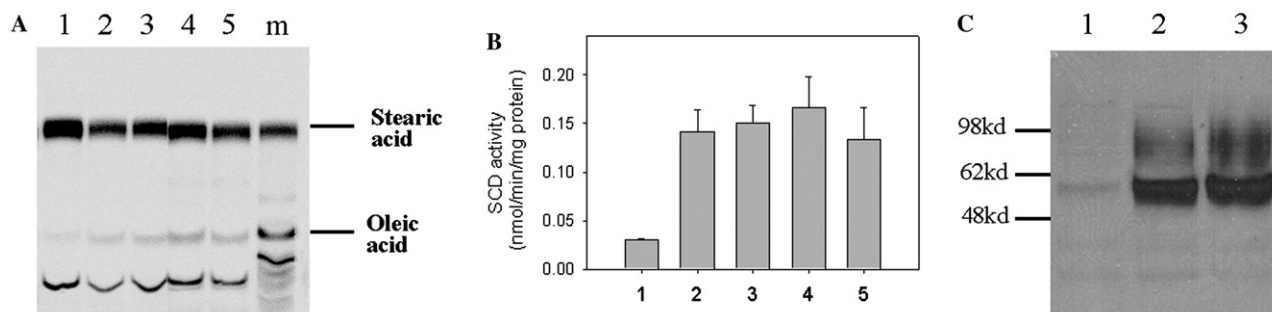


Fig. 2. SCD activity of hSCD1 and hSCD5. (A) Representative images of thin layer chromatography (TLC) plates of SCD reaction from microsomal fraction of 293 cells transfected with pcDNA3 (lane 1), pcDNA3-hSCD1 (lane 2), pEGFP-hSCD1 (lane 3), pcDNA3-hSCD5 (lane 4), and pEGFP-hSCD5 (lane 5).  $^{14}\text{C}$ -labeled stearic acid and oleic acid were also loaded as marker (m). (B) Calculated SCD activities with mean and standard deviations calculated from three independent experiments. Lane assignment is the same as in (A). (C) Western blot analysis of GFP-hSCD5 and GFP-hSCD1 fusion proteins. Microsomal fractions (30  $\mu\text{g}$ ) from mock-transfected (1), pEGFP-hSCD5 (2), and pEGFP-hSCD1 (3) 293 cells were separated on SDS gel and probed with anti-GFP antibody. The GFP-hSCD5 and GFP-hSCD1 fusion proteins were detected as a single band at 58 kDa.

some fraction prepared from 293 cells transfected with hSCD1, hSCD5, GFP-hSCD1, and GFP-hSCD5 displayed similar desaturase activity towards stearoyl-CoA. These data suggest that hSCD5 encodes a functional delta 9 desaturase.

Immunofluorescent microscope study was also performed to determine the subcellular localization of hSCD5. As shown in Fig. 3, both GFP-hSCD1 and GFP-hSCD5 displayed endoplasmic reticulum (ER) staining. This staining pattern was similar to that of a known ER membrane protein, calnexin. Therefore, we

concluded that hSCD5 is similar to hSCD1 in its desaturase activity and subcellular localization.

#### Expression of hSCD1 and hSCD5 in human tissues

To determine the tissue distribution of hSCD5, we designed specific real-time RT-PCR primers and probes for hSCD1 and hSCD5. Quantitative RT-PCR was carried out using RNA from different human adult and fetal tissues. Similar to mSCD1, hSCD1 expression was detectable in several adult tissues with the highest in liver and

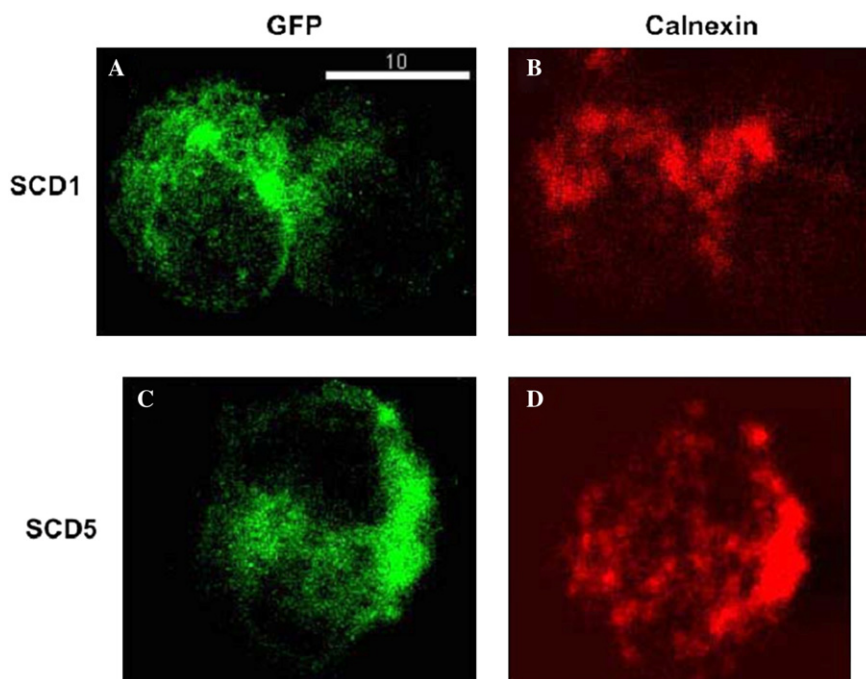


Fig. 3. Confocal micrographs of the HEK-293 cells transfected with pDGFP-hSCD1 (A,B) or pEGFP-hSCD5 (C,D). Both SCD1 and SCD5 were tagged with GFP (green). The same cells were also stained with antibody against calnexin (B,D). Dual channel recording of fluorescent signals from the cells was carried out simultaneously and saved in two separate files. (For interpretation of the references to color in this figure legend, the reader is referred to the web version of this paper.)

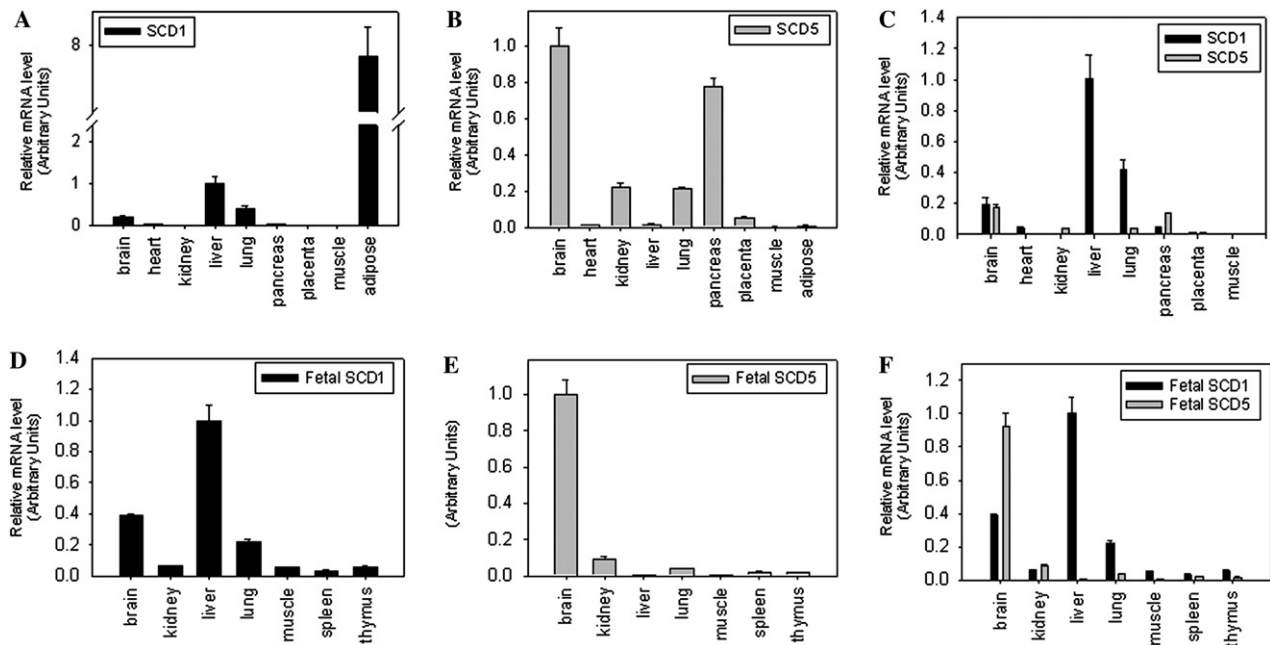


Fig. 4. Semi-quantitative real-time RT-PCR analysis of hSCD1 and hSCD5 mRNA in human tissues. (A) Histogram shows the relative mRNA level of hSCD1 in adult human tissues with the mRNA level in liver as 1. (B) Relative mRNA level of hSCD5 in adult human tissues with the mRNA level in brain as 1. (C) Comparative mRNA level of hSCD1 versus hSCD5 in adult human tissues with the mRNA level in liver as 1. (D) Relative mRNA level of hSCD1 in fetal human tissues with the mRNA level in fetal liver as 1. (E) Relative mRNA level of hSCD5 in fetal human tissues with the mRNA level in fetal brain as 1. (F) Comparative mRNA level of hSCD1 versus hSCD5 in fetal human tissues with the mRNA level in fetal liver as 1.

adipose tissue (Fig. 4A). The hSCD1 mRNA level in adipose tissue is approximately sevenfold higher than in liver. In contrast, the highest mRNA levels of hSCD5 were detected in adult brain and pancreas (Fig. 4B). In adult brain, equivalent levels of hSCD1 and hSCD5 mRNA were detected (Fig. 4C). In the fetal human tissues, the highest hSCD1 mRNA level was detected in fetal liver (Fig. 4D) and the highest hSCD5 mRNA level was detected in brain (Fig. 4E). In the fetal brain, hSCD5 mRNA is twofold more abundant than the hSCD1 (Fig. 4F).

## Discussions

Four SCD isoforms have been identified and characterized in the mouse. So far, only one human SCD isoform has been well characterized. In the current study, we report the identification and characterization of a novel human SCD isoform, hSCD5. Human SCD5 was previously cloned in the chromosome inversion site in a family with cleft lip and was named as ACOD4 (AF389338) due to its homology with other mammalian acyl-CoA desaturases [14]. Here we show that ACOD4 encodes a functional delta 9 desaturase and is localized on ER membrane. Using quantitative RT-PCR method, we show that the highest expression of hSCD5 was detected in the brain and pancreas. In contrast, the highest hSCD1 expression was detected in the liver and adipose tissue, which is similar to its mouse orthologue, mSCD1.

In the NCBI database, ACOD4 was named as SCD4. However, ACOD4 shares only 54.4% identity to mSCD4 at the amino acid level. In contrast, hSCD1 shares 84.8% identity to its mouse orthologue, mSCD1. In fact, hSCD1 shares about 85% identity to all four mouse SCD isoforms as well as rat SCD1 and rat SCD2. All four mouse SCD genes are located in a 200 kb stretch on mouse chromosome 19. It is suggested that all the four mouse SCD genes are derived from tandem gene duplication events [13]. Human SCD1 gene is localized on chromosome 10 and there are no other SCD genes on human chromosome 10, suggesting that the gene duplication event similar to mouse SCD genes did not occur in humans. ACOD4 gene is localized on human chromosome 4. The four mouse SCD isoforms share much less homology to ACOD4 than to hSCD1. Additionally, no expression of ACOD4 was detected in human heart whereas mSCD4 expression is limited to the heart. These data suggest that ACOD4 encodes a distinct stearoyl-CoA desaturase, rather than the human orthologue of mSCD4. Therefore, we named it hSCD5.

Interestingly, extensive BLAST search in the mammalian nucleotide databases revealed potential hSCD5 orthologues in two new world primates, chimpanzee and orangutan. No orthologue of hSCD5 was found in mouse. Considering the fact that mouse genomic sequence is complete, it is likely that hSCD5 orthologue does not exist in mouse. The genomic sequences for

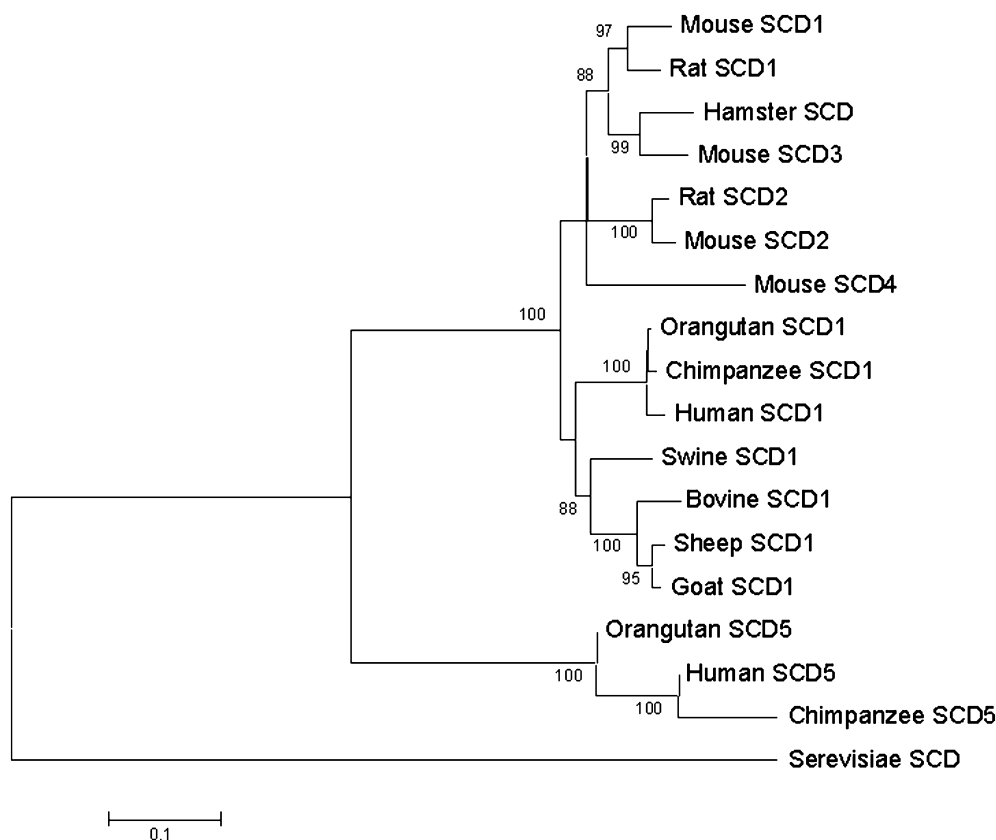


Fig. 5. Phylogenetic tree of mammalian SCD isoforms. The scale bar indicates the unit of amino acid Poisson distance. The percentage bootstrap values are indicated on the branches leading to the clusters. Only bootstrap values larger than 85% are shown. The budding yeast SCD protein is used as an out-group to root the tree.

other domestic animals, such as bovine and canine, are not complete. It is not clear at this point if hSCD5 orthologue exists in these animals.

There are two hypotheses to explain the origin of SCD5. The first hypothesis is that SCD5 existed in all mammals originally but somehow got lost during evolution in certain species, such as rodents. Alternatively, SCD5 might be acquired only in primates later during evolution, thus it is primate specific. Phylogenetic analysis of all available mammalian SCD isoforms (Fig. 5) supports the first hypothesis. Our tree showed that all four mouse SCD isoforms are closely related. This supports the notion that they arrive through recent gene duplication events. It is likely that these gene duplications occurred after the divergence of small rodents from other mammals but before mouse and rat diverged. On the other hand, hSCD5 is closely related to the other two primate SCD5 but quite distant from all rodent SCDs, as well as from SCD1 from human and other mammals. This suggests that SCD1 in mammals, as well as the mSCD2, mSCD3, mSCD4, and rSCD2 share the same ancestral gene. However, the evolution lineage of hSCD5 is created by a single gene duplication event which occurred before the divergence of all mammalian species exam-

ined here. It is worth pointing out that there is a SCD5-like genomic DNA fragment in dogs derived from the canine genomic sequence (data not shown), although cDNA sequence has not been reported. It is likely that as more mammalian species genomic sequences become available, more mammalian SCD5 genes will be found.

SCD plays an important role in lipid metabolism and the regulation of energy expenditure. The existence of multiple SCD isoforms in rodents may be linked to the fact that they generally have a much higher metabolic rate than primates. The highest expression of human SCD5 was detected in adult brain and pancreas. The mouse SCD isoform highly expressed in brain is SCD2 [4]. No study of mouse SCD expression in pancreas was reported. Interestingly, hSCD5 expression is higher in fetal brain than in adult brain. Further study of hSCD5 function would shed light on its role in brain development.

#### Acknowledgments

We thank James Schrementi and Michael Esterman for technical assistance.

## References

- [1] B. Behrouzian, P.H. Buist, Fatty acid desaturation: variations on an oxidative theme, *Curr. Opin. Chem. Biol.* 6 (2002) 577–582.
- [2] P. Sperling et al., The evolution of desaturases, *Prostaglandins Leukotr. Ess. Fatty Acids* 68 (2003) 73–95.
- [3] B. Behrouzian, P.H. Buist, Mechanism of fatty acid desaturation: a bioorganic perspective, *Prostaglandins Leukotr. Ess. Fatty Acids* 68 (2003) 107–112.
- [4] J.M. Ntambi, M. Miyazaki, Recent insights into stearoyl-CoA desaturase-1, *Curr. Opin. Lipidol.* 4 (3) (2003) 255–261.
- [5] P. Cohen, J.M. Friedman, Leptin and the control of metabolism: role for stearoyl-CoA desaturase-1 (SCD-1), *J. Nutr.* 134 (9) (2004) 2455S–2463S.
- [6] P. Dobrzyn et al., Stearoyl-CoA desaturase1 deficiency increases fatty acid oxidation by activating AMP-activated protein kinase in liver, *Proc. Natl. Acad. Sci. USA* 101 (17) (2004) 6409–6414.
- [7] M. Miyazaki et al., The biosynthesis of hepatic cholesterol esters and triglycerides is impaired in mice with a disruption of the gene for stearoyl-CoA desaturase1, *J. Biol. Chem.* 275 (39) (2000) 30132–30138.
- [8] P. Cohen et al., Role for stearoyl-CoA desaturase-1 in leptin-mediated weight loss, *Science* 297 (5579) (2002) 240–243.
- [9] Y. Wang, B. Kurdi-Haidar, J.F. Oram, LXR-mediated activation of macrophage stearoyl-CoA desaturase generates unsaturated fatty acids that destabilize ABCA1, *J. Lipid Res.* 45 (5) (2004) 972–980.
- [10] Y. Sun et al., Stearoyl-CoA desaturase inhibits ATP-binding cassette transporter A1-mediated cholesterol efflux and modulates membrane domain structure, *J. Biol. Chem.* 278 (2003) 5813–5820.
- [11] A.D. Attie et al., Relationship between stearoyl-CoA desaturase activity and plasma triglycerides in human and mouse hypertriglyceridemia, *J. Lipid Res.* 43 (11) (2002) 1899–1907.
- [12] R.R. Brenner et al., Desaturase activities in rat model of insulin resistance induced by a sucrose-rich diet, *Lipids* 38 (2003) 733–742.
- [13] M. Miyazaki et al., Identification and characterization of murine SCD4, a novel heart-specific stearoyl-CoA desaturase isoform regulated by leptin and dietary factors, *J. Biol. Chem.* 278 (36) (2003) 33904–33911.
- [14] S. Beiraghi et al., Identification and characterization of a novel gene disrupted by a pericentric inversion inv(4)(p13.1q21.1) in a family with cleft lip, *Gene* 309 (2003) 11–21.
- [15] F.S. Heinemann, J. Ozols, Stearoyl-CoA desaturase, a short-lived protein of endoplasmic reticulum with multiple control mechanisms, *Prostaglandins Leukotr. Ess. Fatty Acids* 68 (2003) 123–133.
- [16] S. Kumar et al., MEGA2: molecular evolutionary genetics analysis software, *Bioinformatics* 17 (12) (2001) 1244–1245.
- [17] J.D. Thompson, D.G. Higgins, T.J. Gibson, CLUSTAL W: improving the sensitivity of progressive multiple sequence alignment through sequence weighting, position-specific gap penalties and weight matrix choice, *Nucleic Acids Res.* 22 (1994) 4673–4680.
- [18] N. Saitou, M. Nei, The neighbor-joining method: a new method for reconstructing phylogenetic trees, *Mol. Biol. Evol.* 4 (4) (1987) 406–425.
- [19] B. Efron, E. Halloran, S. Holmes, Bootstrap confidence levels for phylogenetic trees, *Proc. Natl. Acad. Sci. USA* 93 (23) (1996) 13429–13441.